RSC Advances

PAPER

Cite this: *RSC Adv.*, 2020, **10**, 32225

Polymer-dispersed liquid-crystal-based switchable glazing fabricated *via* vacuum glass coupling†

Naila Nasir, Hyeryeon Hong, Malik Abdul Rehman, Sunil Kumar and Yongho Seo *

Received 7th July 2020
Accepted 17th August 2020

DOI: 10.1039/d0ra05911k

rsc.li/rsc-advances

Polymer-dispersed liquid crystals (PDLCs) exhibiting transmittance switching are utilized for preserving energy and protecting privacy. Here we prepared a typical PDLC mixture from a commercially available polymer and liquid crystal with nano-beads. A wire-bar coater was used to coat the PDLC mixture on indium-tin-oxide-coated glass, and a PDLC cell was assembled by coupling another glass in a vacuum, instead of a polymer film. Uniform glass-based PDLCs were fabricated successfully with an area of 15×15 cm^2, while an injection process with capillary action was not available for this large-scale device fabrication. The switching behavior of the cells was characterized by ramping the AC voltage, and a transmittance change of ~70% was measured. In a typical roll-to-roll process, only flexible polymer films have been used in lamination, in which deterioration in transparency occurs over the course of time, reducing the efficiency. In this study, to improve the optical properties, PDLC switchable glazing is fabricated directly onto glass substrates instead of onto plastic polymers. This PDLC switchable glazing, exhibiting low haziness and wide-angle vision, can be fabricated at a large scale by a vacuum-coupling process, with potential use as glass windows for energy-efficient buildings.

1. Introduction

Liquid crystal (LC) is an eccentric state of matter whose properties lie in between typical liquid and solid states.[1,2] The mobility and orientational order in a liquid crystal balance each other.[3,4] Polymer-dispersed liquid crystals (PDLCs), a combination of liquid crystals and polymers, have been invented and used in various electro-optical applications since the 1980s.[5] PDLCs can be depicted as a Swiss-cheese structure of polymer in which micro-sized liquid crystals fill in the holes of a continuous polymer matrix.[6–8] The LC and polymer are mixed together forming a homogenous solution and laminated with two transparent substrates, forming the PDLC cell. The distinctive behavior of a PDLC is a consequence of these tiny micrometer-sized LC droplets.[9–11] By virtue of their electro-optic behavior, PDLCs have a wide range of applications, including projection systems, holographic films, flat-panel displays, micro-lens arrays, and switchable glazing.[12–16] Among these applications, the use of PDLCs film for manufacturing switchable glazing is ever-expanding in architectural and automotive sunroofs, skylights, and windows. The wellbeing of the residents of buildings and energy consumption in the built environment is significantly influenced by windows. PDLC switchable glazing can adjust solar radiation for buildings, reduce heating and cooling energy, and increase the annual indoor illuminance ratio. The application of switchable glazing is not limited to the built environment; the interior temperature of automobiles can also be maintained and growing conditions in greenhouses can be improved. Several companies and university groups have been engaged in designing switchable glazing with high contrast ratios, low haziness, enhanced stability and low switching time.[12,17–19] Commercial PDLC devices should possess optimal and superior characteristics, including enhanced stability and response time, and reduced driving voltage. These characteristics can be attained by carefully controlling the composition of the raw materials. The LCs should exhibit higher optical birefringence, and the polymer should have transparency, mechanical strength, and be chemically inert to the LC. The LC and polymer should be miscible with each other in the liquid state and immiscible in the solid state with matching refractive indexes.[9]

The phase separation process can be controlled in order to obtain various morphologies of LC droplets dispersed in polymer film, as required for different applications. Phase separation can be induced by various methods such as polymerization-induced phase separation (PIPS), thermally induced phase separation, and solvent-induced phase separation. PIPS has already been studied intensively by others, as it is used widely for the production of functional materials.[20,21] In PIPS, the homogeneous solution of LC and polymer are cured by ultraviolet light source, whereby the LC phase is separated from the polymer chain, forming droplets while the polymer lengthens.[22–24] In this work, we adopted PIPS as it is a functional method producing uniform and stable PDLC films. After preparing the PDLC cell, it was cured by an ultraviolet (UV) light

Department of Nanotechnology & Advanced Materials Engineering and HMC, Sejong University, Seoul 05006, Republic of Korea. E-mail: yseo@sejong.ac.kr

† Electronic supplementary information (ESI) available. See DOI: 10.1039/d0ra05911k

source, as in the PIPS process, and the LC molecules formed droplets within the polymer matrix. The LC droplets grew until the polymerization was completed, and the PDLC film was solidified. The size of the LC droplets depends on the concentration of the LC component, the UV light intensity, and the curing temperature.[25,26]

In this paper, we introduce a simple and cost-effective method to prepare PDLC switchable glazing directly on glass substrates *via* vacuum glass coupling on a large scale. Previously, PDLC switchable glazing have been prepared by the typical roll-to-roll process. In this process, PDLC film is laminated onto plastic sheet, which is then attached to a rigid glass forming the PDLC window. However, plastic degrades slowly with the passage of time due to atmospheric affects. The ultraviolet rays make it yellowish, shattering the physical appearance of the glazing. Moreover, the plastic sheet placed between the glass substrates also reduces the transmittance, reducing the efficiency of the glazing. Compared to plastic, glass is much more durable, as it is chemically inert and able to withstand high temperature. However, it is impossible to laminate PDLC film directly onto glass substrates using a roll-to-roll process because the glass is not flexible. Thus, we employed a coating technique to fabricate homogeneous and uniform PDLC film directly onto an indium-tin-oxide (ITO)-coated glass substrate to enhance the transmittance of the PDLC glazing. Although small-sized PDLC glass with high transmittance has been prepared by other groups using an injection process or capillary action, these methods are limited to a small-sized cell and are not scalable.[27–29] We demonstrated a PDLC glazing with an area of 15 × 15 cm^2 using wire-bar coating and coupling in a vacuum, preventing the formation of air bubbles in the PDLC device.

2. Experimental

PDLC film composition

In this work, commercially prepared liquid crystal, E7, was used to fabricate the PDLC film. E7 is extensively used in making PDLC film as it sustains anisotropic behavior over a wide temperature range and has high birefringence. E7 is a mixture of 4-pentyl-4′-cyanobiphenyl (51%), 4-heptyl-4′-cyanobiphenyl (25%), 4-octyloxy-4′-cyanobiphenyl (16%), and 4-pentyl-4′-cyanobiphenyl (8%) (see ESI Fig. S1†) with ordinary and extraordinary refractive indexes of 1.521 and 1.746, respectively.[30] A UV-curable adhesive (NOA65, Norland Optical Adhesive) was used as a starting material for the polymer with a refractive index of 1.524. NOA65 cures rapidly when exposed to UV light with a maximum absorption range of 350–380 nm wavelength. The thickness of the polymer and the UV light intensity affect the curing speed. Beside LC and polymer, silicon dioxide (SiO_2) nanoparticles in white powder form were also added. The SiO_2 nanoparticles, purchased from Nanografi, have a purity of 97.3 wt% and average size 16 nm, and are coated with 2 wt% silane. The particle size was confirmed by the scanning electron microscopy (SEM) image obtained by dissolving SiO_2 nanoparticles in ethanol (see ESI Fig. S2†) (More details regarding the nanoparticles are in the ESI Table S1†). The incorporation of SiO_2 nanoparticles (NPs) increases the viscosity of the PDLC mixture to improve the uniformity of the film thickness in the coating process.[27–29,31] Moreover, NPs speeded up the curing process, as NPs play a role of a scattering center for UV due to the refractive index mismatch between the NP and the monomer.

Fabrication

We prepared the PDLC mixture in vials by mixing LC E7, polymer NOA65, and white powdered nanoparticles of SiO_2. The weight% of each chemical added in the PDLC mixture was chosen after many trials. The composition with the best results contained LC, NOA65, and SiO_2 with a weight% of 60%, 35%, and 5%, respectively. The mixture was stirred at room temperature for 1 hour using an homogenizer (Ultra Turrax, IKA Ltd) at 30 000 rpm. To prepare a homogeneous mixture without undissolved particles, stirring was done at a higher temperature (130 °C) as well. After heating, the mixture was also kept in a vacuum for half an hour so that the SiO_2 particles were completely dissolved in LC and NOA65, resulting in the formation of a uniform and homogeneous PDLC mixture. The mixture was coated on 15 cm × 15 cm ITO-coated glass (sheet resistance: 7 Ω sq^{-1}, Wooyang GMS, South Korea). Before coating, the ITO-coated glass was carefully cleaned to remove impurities and dust particles by sonication with acetone, isopropyl alcohol, and distilled water. The PDLC mixture was coated onto ITO-coated glass using a wire-bar coater, as shown in Fig. 1a. The wire-bar coater consists of a rectangular board and a metallic bar to roll over the glass substrate. A metal wire is wound around the bar, thus making grooves. The diameter of the grooves determines the amount of PDLC passing through the grooves. The glass substrate is fixed onto the rectangular board. The bar rolls over, fabricating a uniform PDLC film on the glass substrate. To attach the top glass to the PDLC-coated bottom glass under vacuum, we designed a special coupling device, as shown in Fig. 1b. It consists of a rectangular plate with four hinges at the corners. The PDLC-coated glass is placed at the bottom of the plate, while the top glass is placed on the hinges separating the top and bottom glass (∼1 cm). The hinges are connected to rotating shafts, where permanent magnets are attached. This structure is placed inside a vacuum desiccator. A vacuum was created in the vacuum chamber up to ∼0.1 torr for 1 hour. By bringing some external magnets close to the internal magnets, the rotating shafts inside the chamber were rotated using the magnetic force between the magnets. As a result, the hinges were moved away, dropping the top glass onto the bottom glass. Afterwards the chamber was purged for the top and bottom glasses to form a PDLC cell, as shown in Fig. 1c (see ESI Fig. S3† for the apparatus used in the fabrication of the PDLC device). The PDLC cell was then cured for 15 minutes using an ultraviolet light source with a mercury lamp (1 kW power) at 23 cm distance from the lamp, with an intensity of 95 mW cm^{-2}.

Dispersion of nanoparticles in the mixture

The SiO_2 nanoparticles should be completely dissolved in the PDLC mixture with LC and NOA65. Otherwise, the undissolved particles will result in non-uniform films causing

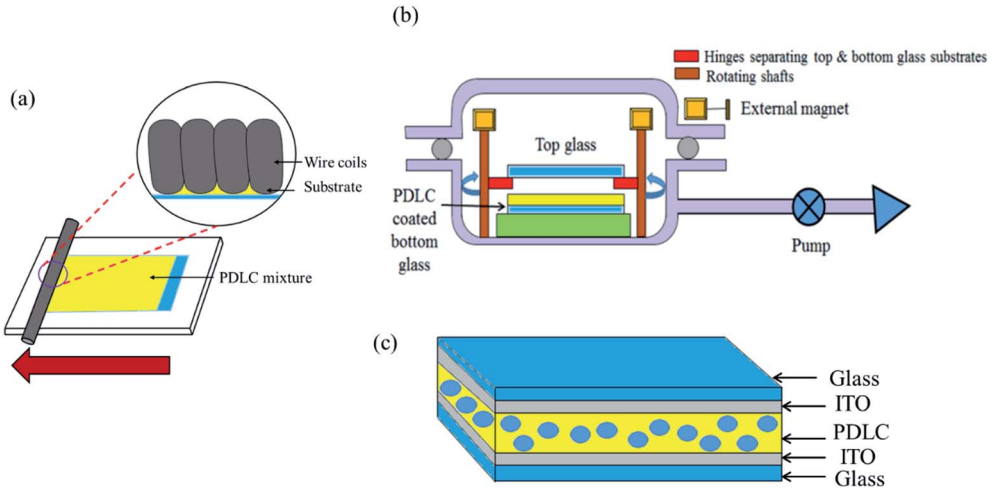

Fig. 1 (a) A wire-bar coater was used to coat the PDLC mixture. (b) In a vacuum chamber the vacuum assembly holds the top and bottom glasses for vacuum coupling. (c) The structure of the PDLC cell is shown.

inhomogeneous switchable behavior, and not fulfilling the criteria required for a commercial product. Thus, we examined the mixture at different stages using SEM in order to ensure its homogeneity. SEM images were obtained after coating the mixture on a silicon substrate. Fig. 2a shows the SEM image of the mixture status after it was stirred at room temperature for 1 hour. Some undissolved particles were observed in the mixture, as shown in the inset. Fig. 2b shows the state when the mixture was stirred on a hot plate at 130 °C for 1 hour. It is observed that the homogeneity of mixture was improved, with less undissolved particles compared to the image in Fig. 2a. Then, the PDLC mixture was stirred at 130 °C and kept in vacuum, and the stirring-vacuum process was repeated for 2 hours. Fig. 2c shows the result, exhibiting no undissolved particles left behind. This completely dissolved PDLC mixture was used for the subsequent PDLC cell fabrication.

Uniformity of film thickness

The PDLC mixture coated onto glass substrates using a wire-bar coater was shown to be a highly uniform film. The standard wire-bar #10 was used to coat the film at a thickness of ~23.0 μm. After UV curing, the film thickness uniformity was measured using a three-dimensional (3D) coordinate measuring machine (600XP, VIEW). The thickness of the PDLC was measured at 15 points on the film. Then, the average value of the thickness was obtained as 22.0 μm, which is close to the target value with a standard deviation of 0.95 μm, thus confirming the uniformity.

3. Results and discussions

Switching behavior of PDLC

PDLC shows a switching behavior between the opaque state and the transparent state, as illustrated in Fig. 3. The directors (average direction of the LC molecules) inside the LC droplets are randomly distributed when no field is applied (the off state). In this state, the effective refractive index of the LC and the refractive index of the polymer are mismatched, scattering the incident light and rendering the PDLC a milky white in appearance. When an external field is applied, the directors within the LC droplets reorient along the field, and the incident

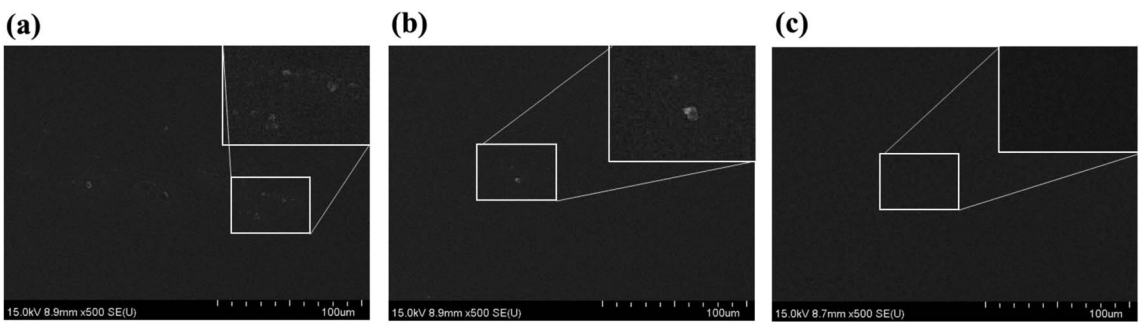

Fig. 2 SEM images show states of the PDLC mixtures: (a) after stirring at room temperature, (b) after stirring at the hot plate, and (c) after stirring at the hot plate and under vacuum. The insets are the magnified images showing any undissolved clusters of nanoparticles.

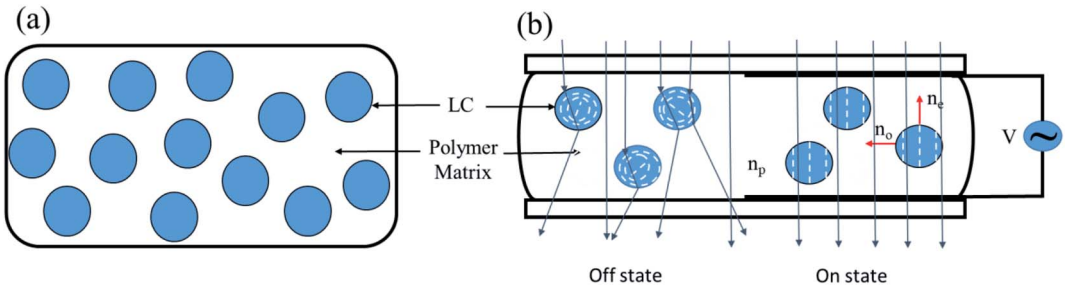

Fig. 3 (a) Liquid-crystal droplets are dispersed in the polymer matrix. (b) The switching mechanism of PDLC is illustrated dependent on the applied electric field.

light passes through it without scattering, since the ordinary refractive index of the LC matches the refractive index of the polymer, causing PDLC to have a transparent appearance. The strength of the electric field required for switching from opaque to transparent state depends upon the shape, size, and dielectric anisotropy of the LC droplets.[32]

The switching behavior of the PDLC devices was characterized at different voltages using an AC voltage driver at 60 Hz. The PDLC device appeared opaque in the off state, scattering light, as shown in Fig. 4a. The PDLC cell was completely homogeneous over the whole area, and no hole or blister was observed, which are commonly generated if the mixture is injected by capillary action, or if the top layer is attached in air. On the other hand, the LC domains were aligned in the direction of the applied field in the on state, and the PDLC became transparent, as shown in Fig. 4b. The change in transmittance $\Delta T = (T_{on} - T_{off})$ between the off and on states was estimated as ~70% using a laser source, a photodiode, and an oscilloscope.

Transmittance depending on incident angle

The optical properties of the PDLC cells fabricated on ITO glass were compared with a commercial PDLC film made of poly(ethylene terephthalate) (PET) as a reference sample, as shown in Fig. 5a. Transmittance *versus* voltage curves for the glass-based PDLC (g-PDLC) were measured in comparison to the PET-based PDLC (p-PDLC). These curves show the typical behavior of general PDLCs, which are similar to the other samples fabricated under different conditions, in broad outline, as shown in ESI Fig. S4.† In detail, the on-state transmittance for g-PDLC at 0 V was ~6% greater than the reference sample, which is interpreted as being due to the larger LC droplets in the g-PDLC. In the vacuum-coupling process, microbubbles trapped in the mixture could be removed, and phase separation of LC might be facilitated, thus forming larger droplets. Furthermore, the increased LC droplet size decreased the threshold voltage (~10 V) to turn-on. In general, the threshold voltage depends on the droplet size, droplet shape, and anchoring condition of the LC. If the size of the LC is larger, a lower threshold voltage is required, because more LC molecules inside the droplet are less influenced by the anchoring force at the interface between the LC droplet and the polymer. Conversely, the small size of the LC droplet increases the threshold voltage.[7,33,34] The enhanced transmittance was almost saturated with an applied voltage of 60 V, which was similar to the reference sample. As a result, while ΔT of g-PDLC was

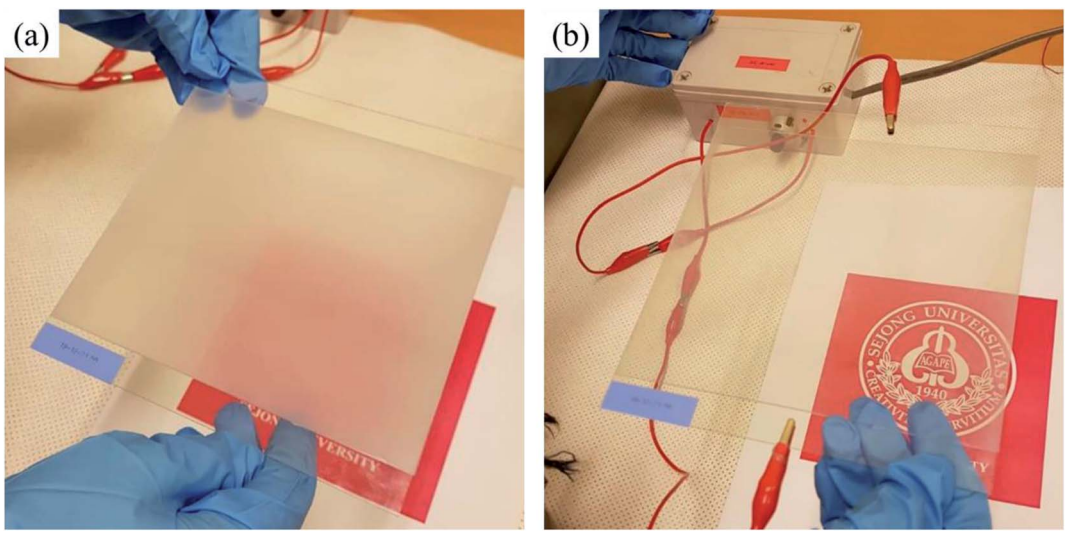

Fig. 4 (a) The PDLC device was opaque in the off state. (b) The PDLC device became transparent in the on state.

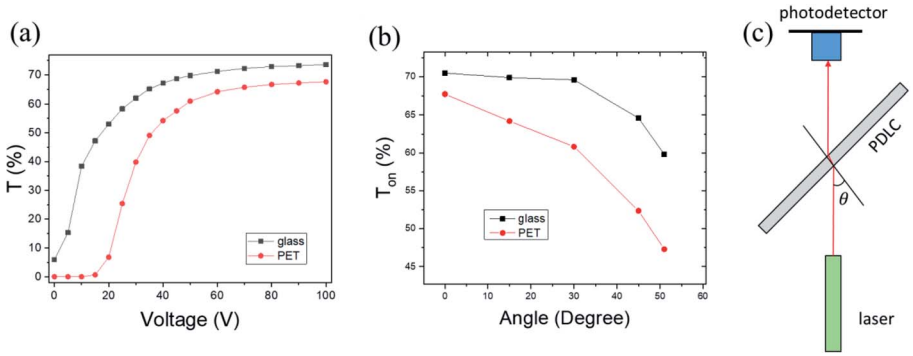

Fig. 5 (a) Transmittance *versus* voltage curves for g-PDLC and p-PDLC. (b) T_{on} *versus* angle curves for g-PDLC and p-PDLC. Transmittance in the on state was measured at different angles θ from 0° to 51°. (c) The schematic shows the tilt-angle-dependent measurement setup.

similar to that of p-PDLC, the whole transmittance of g-PDLC was higher due to the high transparency of the glass.

An angle-dependent transmittance measurement was performed to test the transparency in the tilt-angle view, as shown in Fig. 5c. The incident angle (θ) between the normal direction of the PDLC plane and the laser beam was varied while a driving voltage of 60 V was applied to the PDLC. The transparency of g-PDLC was compared with p-PDLC by rotating the PDLC, as shown in Fig. 5b. While the T_{on} values for the samples were similar at normal incident ($\theta = 0$) beam, a rapid decrease in T_{on} was observed in the p-PDLC. From the tilt-angle results, it was confirmed that g-PDLC is superior, with a wide-angle view, compared to p-PDLC. This effect can be explained by Fresnel equations depending on the incident angle, θ. While the refractive index of PET is 1.575, the refractive index of glass is ~1.52, close to that of NOA65. From the Fresnel equations for unpolarized light, higher reflectance is expected at the interface of a transparent medium with higher refractive index, including air-to-medium and medium-to-air incident events. The rapid decrease in T_{on} near 50° corresponds to the total internal reflection for medium-to-air incident light. The g-PDLC exhibited much higher transmittance than p-PDLC near the total reflection angle, in particular.

Measurement of haziness

The haziness of the PDLC cells fabricated on ITO glass were measured with a commercial PDLC film made of PET as a reference sample, as shown in Fig. 6. Haze factor *versus* voltage curves for g-PDLC were plotted in comparison to the p-PDLC at 0, 50, 60 and 70 V. We observed that the haziness reduces as the applied voltage increases for both g-PDLC and p-PDLC. In the off state (0 V), a maximum haze factor was measured, as the incident light was scattered, giving the PDLC a milky appearance. As voltage is applied, the PDLC becomes transparent, allowing the incident light to pass through, and reducing the haze factor. The off-state haze factor is ~90% for both the g-PDLC and p-PDLC, while the on-state haze factor for g-PDLC is 10% lower than that for p-PDLC, confirming that the g-PDLC fabricated *via* vacuum glass coupling is superior to p-PDLC in terms of transparency. The high haze factor for the p-PDLC on state is attributed to the lower transparency with milky appearance of the polymer compared with the glass.

Response time measurement

A response time measurement was performed as shown in Fig. 7. The measurement was done using a laser source and a photodiode with a pinhole. Fig. 7a and b show, respectively, the transmission response as a function of time when the PDLC device was turned on and turned off. The data show the typical behavior for a short turn-on time (~0.3 ms) and a long turn-off time (~0.1 s). During turn-on the applied electric field aligns the liquid crystals more rapidly because energy is supplied from the external source. On the other hand, during turn-off the transmittance approaches zero slowly, implying that the liquid crystals take longer to return to the disordered state (long turn-off time), as the turn-off process is an energy-dissipating process *via* surface anchoring of LC molecules.[7] These turn-on and turn-off times are typical values, similar to those of

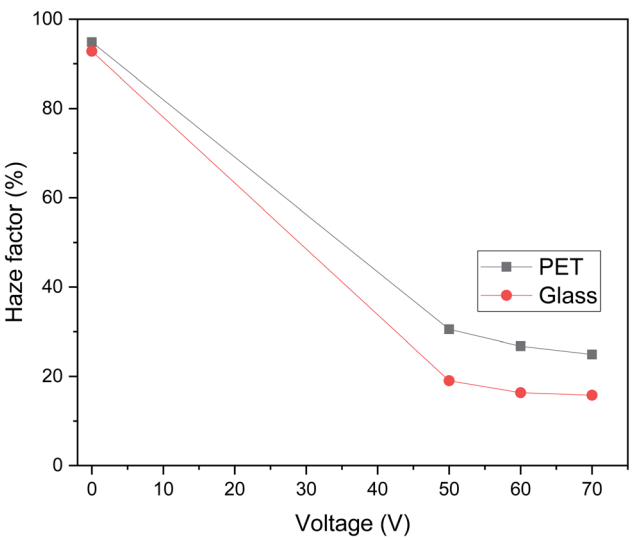

Fig. 6 Haze factor *versus* voltage curve for glass-based PDLC and PET-based PDLC.

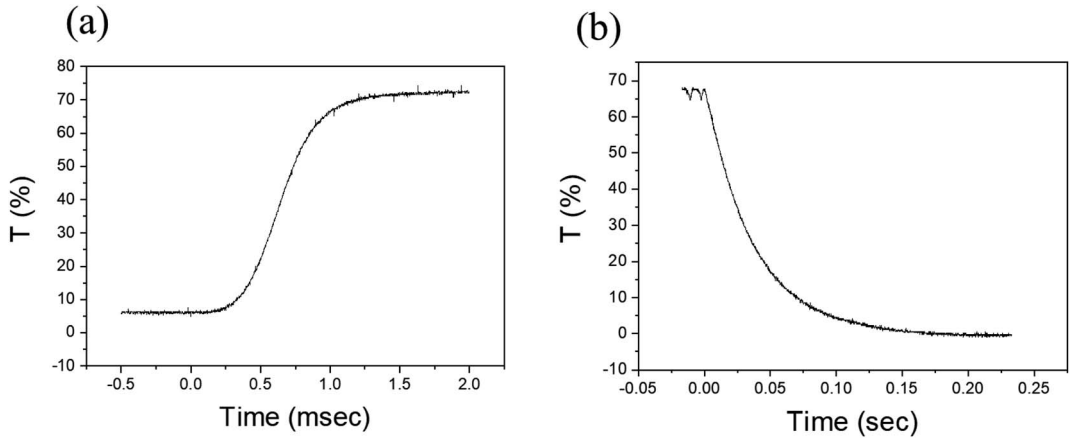

Fig. 7 Time evolution transmittances were recorded in (a) the turn-on process and (b) the turn-off process to estimate the response times.

conventional PDLCs. It can be seen that the vacuum-coupling process does not influence the switching speed of the PDLC.

4. Conclusion

We demonstrated a facile and cost-effective method, so-called "vacuum glass coupling", to fabricate a glass-based PDLC device, as an alternative method for the conventional roll-to-roll process that is available only for flexible substrates. This fabrication method can be applied widely for general solid substrates without limitation of size. This g-PDLC device, fabricated using this simple method, exhibited a high transmittance change with a low driving voltage of 60 V. Furthermore, the high transmittance was sustained at a wide range of tilt angles. This glass-based smart window can be utilized not only for purposes of indoor privacy, but also for energy saving purposes under direct sunlight, as the glass is durable for UV irradiation. Thus, this switchable glazing has significant potential for numerous commercial and industrial applications.

Author contributions

Research design, N. N. and Y. S.; Experiments and data analysis, N. N., H. H., S. K., M. A. R., and Y. S; Paper writing, S. K., and Y. S.

Conflicts of interest

The authors declare no conflicts of interest.

Acknowledgements

This research was supported by the World Class 300 Project (S2561932) of the SMBA, the Korea Institute of Energy Technology Evaluation and Planning (KETEP) and the Ministry of Trade, Industry & Energy of the Republic of Korea (20184030202260), and the National Research Foundation of Korea (NRF) grant funded by the Korea government (MSIT) (NRF-2020R1A6A1A03043435).

References

1 P.-G. De Gennes and J. Prost, *The physics of liquid crystals*, Oxford university press1993.
2 D.-K. Yang and S.-T. Wu, *Fundamentals of liquid crystal devices*, John Wiley & Sons2014.
3 A. Jákli and A. Saupe, *One-and two-dimensional fluids: properties of smectic, lamellar and columnar liquid crystals*, CRC Press, 2006.
4 P. d. Gennes, J. Prost and R. Pelcovits, *The physics of liquid crystals*, Oxford University, Press1995.
5 J. W. Doane, A. Golemme, J. L. West, J. B. Whitehead and B. G. Wu, Polymer Dispersed Liquid-Crystals for Display Application, *Mol. Cryst. Liq. Cryst.*, 1988, **165**, 511–532.
6 S. Kumar, H. Hong, W. Choi, I. Akhtar, M. A. Rehman and Y. Seo, Acrylate-assisted fractal nanostructured polymer dispersed liquid crystal droplet based vibrant colored smart-windows, *RSC Adv.*, 2019, **9**(22), 12645–12655.
7 Y. Kim, K. Kim, K. B. Kim, J. Y. Park, N. Lee and Y. Seo, Flexible polymer dispersed liquid crystal film with graphene transparent electrodes, *Curr. Appl. Phys.*, 2016, **16**(3), 409–414.
8 Y. Kim, D. Jung, S. Jeong, K. Kim, W. Choi and Y. Seo, Optical properties and optimized conditions for polymer dispersed liquid crystal containing UV curable polymer and nematic liquid crystal, *Curr. Appl. Phys.*, 2015, **15**(3), 292–297.
9 M. Mucha, Polymer as an important component of blends and composites with liquid crystals, *Prog. Polym. Sci.*, 2003, **28**(5), 837–873.
10 Y. J. Jeon, Y. Bingzhu, J. T. Rhee, D. L. Cheung and M. Jamil, Application and New Developments in Polymer-Dispersed Liquid Crystal Simulation Studies, *Macromol. Theory Simul.*, 2007, **16**(7), 643–659.
11 Y. Liu and X. Sun, Holographic polymer-dispersed liquid crystals: materials, formation, and applications, *Adv. Optoelectron.*, 2008, (2008), 684349.

12 C. M. Lampert, *Progress in switching windows, Solar and Switching Materials*, International Society for Optics and Photonics, 2001, pp. 95–103.
13 C. M. Lampert, Large-area smart glass and integrated photovoltaics, *Sol. Energy Mater. Sol. Cell.*, 2003, **76**(4), 489–499.
14 G. P. Crawford, *Flexible flat panel display technology*, Wiley Online Library, 2005.
15 T. J. White, L. V. Natarajan, T. J. Bunning and C. Allan Guymon, Contribution of monomer functionality and additives to polymerization kinetics and liquid crystal phase separation in acrylate-based polymer-dispersed liquid crystals (PDLCs), *Liq. Cryst.*, 2007, **34**(12), 1377–1385.
16 A. Elqidrea, R. Meziane and U. Maschke, Kinetics and molecular weight characterization of poly (2-ethylhexyl acrylate) and liquid crystal (5CB) composites, *Mol. Cryst. Liq. Cryst.*, 2011, **547**(1), 128/[1818]–134/[1824].
17 A. Seeboth, J. Schneider and A. Patzak, Materials for intelligent sun protecting glazing, *Sol. Energy Mater. Sol. Cell.*, 2000, **60**(3), 263–277.
18 H. Watanabe, Intelligent window using a hydrogel layer for energy efficiency, *Sol. Energy Mater. Sol. Cell.*, 1998, **54**(1–4), 203–211.
19 G.-S. Kim and S.-H. Hyun, Synthesis of window glazing coated with silica aerogel films *via* ambient drying, *J. Non-Cryst. Solids*, 2003, **320**(1–3), 125–132.
20 A. Matsuyama, Phase separations in mixtures of a liquid crystal and a nanocolloidal particle, *J. Chem. Phys.*, 2009, **131**(20), 204904.
21 S. A. Khadem and A. D. Rey, Theoretical Platform for Liquid-Crystalline Self-Assembly of Collagen-Based Biomaterials, *Front. Phys.*, 2019, **7**, 88.
22 J. L. West, Phase separation of liquid crystals in polymers, *Mol. Cryst. Liq. Cryst.*, 1988, **157**(1), 427–441.
23 N. A. Vaz, G. W. Smith and G. P. Montgomery Jr, A light control film composed of liquid crystal droplets dispersed in an epoxy matrix, *Mol. Cryst. Liq. Cryst.*, 1987, **146**(1), 17–34.
24 A. Golemme, S. Zumer, J. Doane and M. Neubert, Deuterium NMR of polymer dispersed liquid crystals, *Phys. Rev. A*, 1988, **37**(2), 559.
25 E. R. Soule and A. D. Rey, Modelling complex liquid crystal mixtures: from polymer dispersed mesophase to nematic nanocolloids, *Mol. Simul.*, 2012, **38**(8–9), 735–750.
26 I. Dierking, A. Rey, L.-C. Chien, U. Maschke, T. Bunning, S. Morris, D.-K. Yang, H. Furue, E. Soto-Bustamante and P. Rudquist, *Polymer-modified liquid crystals*, Royal Society of Chemistry, 2019.
27 J. Heo, J.-W. Huh and T.-H. Yoon, Fast-switching initially-transparent liquid crystal light shutter with crossed patterned electrodes, *AIP Adv.*, 2015, **5**(4), 047118.
28 V. N. John, S. N. Varanakkottu and S. Varghese, Flexible, ferroelectric nanoparticle doped polymer dispersed liquid crystal devices for lower switching voltage and nanoenergy generation, *Opt. Mater.*, 2018, **80**, 233–240.
29 A. Kumari and A. Sinha, Role of $BaTiO_3$ nanoparticles on electro-optic performance of epoxy-resin-based PDLC devices, *Liq. Cryst.*, 2020, 1–12.
30 P. Oswald and P. Pieranski, *Nematic and cholesteric liquid crystals: concepts and physical properties illustrated by experiments*, CRC press, 2005.
31 X. Yan, Y. Zhou, W. Liu, S. Liu, X. Hu, W. Zhao, G. Zhou and D. Yuan, Effects of silver nanoparticle doping on the electro-optical properties of polymer stabilized liquid crystal devices, *Liq. Cryst.*, 2019, 1–8.
32 J. Kelly, W. Wu and P. Palffy-muhoray, Wavelength dependence of scattering in PDLC films: droplet size effects, Molecular Crystals Liquid Crystals Science Technology Section A, *Mol. Cryst. Liq. Cryst.*, 1992, **223**(1), 251–261.
33 W. B. Li, Y. B. Cao, H. Cao, M. Kashima, L. J. Kong and H. Yang, Effects of the structures of polymerizable monomers on the electro-optical properties of UV cured polymer dispersed liquid crystal films, *J. Polym. Sci., Part B: Polym. Phys.*, 2008, **46**(13), 1369–1375.
34 S. X. Cheng, R. K. Bai, Y. F. Zou and C. Y. Pan, Electro-optical properties of polymer dispersed liquid crystal materials, *J. Appl. Phys.*, 1996, **80**(4), 1991–1995.